



Bacterial Nanotubes as Intercellular Linkages in Marine Assemblages

Nirav Patel^{1*}, Yosuke Yamada² and Farooq Azam¹

¹ Marine Biology Research Division, Scripps Institution of Oceanography, University of California, San Diego, La Jolla, CA, United States, ² Okinawa Institute of Science and Technology Graduate University, Okinawa, Japan

OPEN ACCESS

Edited by:

Tony Gutierrez,
Heriot-Watt University,
United Kingdom

Reviewed by:

Andreas Teske,
University of North Carolina at Chapel
Hill, United States
Jin Zhou,
Tsinghua University, China

*Correspondence:

Nirav Patel
niravpatel215@gmail.com

Specialty section:

This article was submitted to
Aquatic Microbiology,
a section of the journal
Frontiers in Marine Science

Received: 01 September 2021

Accepted: 12 November 2021

Published: 09 December 2021

Citation:

Patel N, Yamada Y and Azam F
(2021) Bacterial Nanotubes as
Intercellular Linkages in Marine
Assemblages.
Front. Mar. Sci. 8:768814.
doi: 10.3389/fmars.2021.768814

Several types of bacterial appendages, e.g., pili and fimbriae, are known for their role in promoting interactions and aggregation with particles and bacteria in the ocean. First discovered in *Bacillus subtilis* and *Escherichia coli*, but novel to marine bacteria, bacterial nanotubes are hollow tubular structures connecting cell pairs that allow for the internal transport of cytoplasmic metabolites across the connecting structure. While the significance of nanotubes in exchange of cytoplasmic content has been established in non-marine bacteria, their occurrence and potential ecological significance in marine bacteria has not been reported. Using multiple high-resolution microscopy methods (atomic force microscopy, scanning, and transmission electron microscopy), we have determined that marine bacteria isolates and natural assemblages from nearshore upper ocean waters can express bacterial nanotubes. In marine isolates *Pseudoalteromonas* sp. TW7 and *Alteromonas* sp. ALTSIO, individual bacterial nanotubes measured 50–160 nm in width and extended 100–600 nm between connected cells. The spatial coupling of different cells via nanotubes can last for at least 90 min, extending the duration of interaction events between marine bacteria within natural assemblages. The nanomechanical properties of bacterial nanotubes vary in adhesion and dissipation properties, which has implication for structural and functional variability of these structures in their ability to stick to surfaces and respond to mechanical forces. Nanotube frequency is low among cells in enriched natural assemblages, where nanotubes form short, intimate connections, <200 nm, between certain neighboring cells. Bacterial nanotubes can form the structural basis for a bacterial ensemble and function as a conduit for cytoplasmic exchange (not explicitly studied here) between members for multicellular coordination and expression. The structural measurements and nanomechanical analyses in this study also extends knowledge about the physical properties of bacterial nanotubes and their consequences for marine microenvironments. The discovery of nanotube expression in marine bacteria has significant potential implications regarding intimate bacterial interactions in spatially correlated marine microbial communities.

Keywords: bacterial nanotubes, linkages, intercellular connections, AFM, physical interactions

INTRODUCTION

Marine microbial communities are comprised cumulatively of extremely abundant (10^{29} estimated bacteria in the global ocean) and diverse cells that shape the biological and biogeochemical landscapes of the oceans through interactions with their biotic and abiotic environments (Azam et al., 1994; Azam and Malfatti, 2007; Flemming and Wuertz, 2019). Numerous microbial associations and interactions drive and regulate carbon and nutrient fluxes in the ocean via the microbial loop through the production, transformation, and remineralization of organic matter. The aggregate of marine microbes' activity is a major force structuring the global ocean ecosystems that varies spatially and temporally. Therefore, a fundamental goal in microbial oceanography is to understand how microbes interact with their organic matter field, including other microbes, and larger organisms – and with what ecosystem consequences.

This is a formidable challenge given the enormous complexity of the organic matter pool in the ocean, the diversity of potential interactions, and the range of spatial scales of influence – from nanometers to the ocean basins. Further, the occurrence of organic matter is compositionally, spatially, and temporally variable with feedbacks to the interacting microbes. The global ocean dissolved organic matter-carbon (DOM-C) inventory is huge, being comparable to the entire atmospheric CO_2 -C pool. Yet, the concentration of readily utilizable DOM is only few tens of μM -C with individual molecular species occurring at sub-pM to nM (Benner and Kaiser, 2003; Wakeham et al., 2003; Kaiser and Benner, 2008; Zark et al., 2017). So, the challenge for pelagic marine bacteria is to grow and persist at the expense of such vanishingly low concentrations of DOM. This has raised the question whether pelagic bacteria gain metabolic and growth advantage by interacting with colloids and particulate detritus to solubilize them, thus generating microscale loci of high DOM. Furthermore, submicron-sized colloids, present at $\sim 10^8$ particles mL^{-1} in ambient seawater (Wells and Goldberg, 1991) and likely even greater in phycospheres and detritospheres, might attach to bacterial surface and appendages, generating nanoscale hotspots of organic matter directly on cell surface.

Marine bacteria also interact with co-occurring bacteria as sources of organic nutrients and energy employing a variety of strategies and mechanisms. Bacteria are highly abundant in surface seawater ($\sim 10^6$ mL^{-1}) and on marine snow ($\sim 10^9$ mL^{-1}) so bacteria-bacteria separation on average is ~ 100 μm in the surface ocean and ~ 10 μm on marine snow. Some bacterial interactions involve the coordination of biological activity and phenotypic expression in groups of bacteria due to quorum sensing. Bacteria-bacteria antagonistic interactions involving several types of secretion systems have also been reported in marine bacterial communities (Russell et al., 2014; Green and Mecsas, 2016; Klein et al., 2020). Other contact-dependent mechanisms involving physical intercellular connections (e.g., pili and microbial nanowires) for bacteria-bacteria interactions and activity have been extensively studied. Bacterial pili promote bacterial adhesion to surfaces; type IV pili translocate biomolecules between two connected cells (Pelicic, 2008; Lukaszczyk et al., 2019). *Geobacter sulfurreducens* and *Shewanella oneidensis* produce electrically conductive pili to connect cells

over micrometer distances with the capability of extracellular electron transfer for mediating cell-cell communication (Sure et al., 2016). *S. oneidensis* forms nanowires ~ 10 nm in diameter from outer membrane extensions that connect cells for direct electron transfer (Pirbadian et al., 2014). Extracellular bridges have been observed in *Myxococcus xanthus* as outer membrane vesicles fuse into appendages (Remis et al., 2014). Similar appendages form in marine flavobacteria due to “pearling” of membrane vesicles 50–80 nm in diameter and 80–100 nm in length forming chain-like appendages 0.5–2 μm long (Fischer et al., 2019).

We have been testing the hypothesis that some marine bacterial surface appendages might additionally serve to capture and concentrate colloidal organic matter from seawater and the bacterium could then enzymatically solubilize and utilize these concentrates of colloidal particles (Patel et al., in preparation). During this study employing atomic force microscopy in order to visualize colloids associating with bacterial appendages in real time, we noticed intercellular connections among bacterial cells involving surface appendages that did not match the characteristics of previously described surface appendages of marine bacteria. However, these intercellular appendages were similar to bacterial nanotubes first discovered in *Bacillus subtilis* and *Escherichia coli* (Dubey and Ben-Yehuda, 2011). These authors named the appendages “bacterial nanotubes” after analogous structures like tunneling nanotubes that had previously been reported in eukaryotic cells; these dynamic connections facilitate exchange of intracellular contents in various cell types (e.g., neuronal cells, endothelial cells, myogenic satellite cells) (Gousset et al., 2009; Tavi et al., 2010; Astanina et al., 2015; Alarcon-Martinez et al., 2020).

Dubey and Ben-Yehuda discovered that *B. subtilis* and *E. coli* can produce intercellular nanotubes, where adjacent cells form connections with hollow tubular structures that mediate direct transfer of biomolecules (Dubey and Ben-Yehuda, 2011). They showed that bacterial nanotubes are fundamentally distinct from other physical microbial connections involving extracellular appendages, e.g., pili, flagella, and elongated membrane extensions. They described two types of nanotubes: thick tubes connecting distal cell pairs and thin tubes 30–130 nm wide and up to 1 μm long arrayed to connect cells (Dubey and Ben-Yehuda, 2011). Nanotubes were functioning as conduits for the intercellular exchange of cytoplasmic material, including plasmids and proteins, between neighboring cells (Dubey et al., 2016). Nanotubes can also connect interspecies pairs in mixed cultures of *B. subtilis*, *E. coli*, and *Staphylococcus aureus*, increasing the potential for complex cell interactions within a mixed microbial community (Dubey and Ben-Yehuda, 2011). Pande et al. (2015) found that interspecies nanotubes can accommodate mutually beneficial bidirectional molecular transport in co-cultured auxotrophic mutants of *E. coli* and another terrestrial bacterium *Acinetobacter baylyi* under nutrient limiting conditions. Bacterial nanotubes can directly deliver tRNase toxin and cell wall hydrolases into recipient cells as an asymmetric competitive or cooperative microbial strategy (Stempler et al., 2017; Baidya et al., 2020). As direct connections and conduits for intercellular exchanges of macromolecules, bacterial nanotubes offer

opportunities for coordinated biological activity within groups of microbial cells.

Our finding of nanotube expression in marine bacteria prompted us to begin to address their influence on how bacteria interact with the organic matter (including other bacteria) and on the microscale physical structure of pelagic marine ecosystems. Bacterial nanotubes could be a novel microbial strategy for creating and/or exploiting DOM hotspots in the pelagic ocean, by establishing hollow connections between cells and enabling intercellular exchanges of cytoplasmic macromolecules, offering interesting opportunities for coordinated biological activity. We report first observations of intercellular nanotubes in marine bacterial isolates and within natural marine assemblages using atomic force microscopy (AFM).

The application of AFM on live cells enabled us to visualize these structures that have escaped prior observation, and the potential to probe their biomechanical properties and functionality due to AFM force application and sensing capabilities. Using complementary microscopy techniques AFM, SEM, and TEM, we show these structures are hollow and could accommodate the transport and exchange of internal cellular material. We also found additional types of contact-dependent linkages complementary to bacterial nanotubes in tethering bacteria into networks, sometimes between morphologically different cells. Our findings add to understanding of bacterial interactions with other bacteria, pertaining to the potential density and diversity of nanotubes and other intercellular connections in bacterial assemblages.

MATERIALS AND METHODS

Bacterial Cultures

Samples with natural marine assemblages were prepared from seawater collected off Ellen Browning Scripps Memorial Pier (San Diego, CA, United States). Samples (100 mL) were filtered upon a 0.2- μm polycarbonate filters and resuspended in 10 mL of 0.2- μm filtered autoclaved seawater (FASW) and enriched with Marine Broth 2216 liquid medium (Becton, Dickinson and Company, MD, United States) to adjust the final concentration to 1 or 10% marine broth. Enriched seawater cultures were incubated on a shaker (150 rpm) at room temperature for 20 h before sample preparation for AFM without any further modification.

Marine bacterial isolates *Alteromonas* sp. ALTSIO, *Pseudoalteromonas* sp. TW7, and α -proteobacteria isolates sp. La5 and La6 (isolated from seawater collected from Scripps Pier) were cultured in Marine Broth 2216 liquid medium. Bacterial cells were sampled from cultures at mid-exponential phase and centrifuged at 3,000 g for 5 min. Pelleted cells were resuspended in FASW in 40–50% of the initial volume and used in sample preparations.

Cell Sample Preparation for Atomic Force Microscopy

Cleaned glass coverslips were treated with poly-D-lysine by placing a 10 μL droplet of a 1 mg/ml solution between a pair

of coverslips and separating to air dry. A sample region for cells was demarcated with a hydrophobic barrier by outlining a circle with a liquid blocker PAP pen. A volume of 200 to 250 μL of cell suspension was deposited upon the poly-D-lysine-coated glass coverslip and incubated at room temperature for 30 min to 1 h. The cell suspension was exchanged for fresh FASW buffer using a pair of syringes simultaneously to gently replace the media and then promptly fixed with 20 μL of 37% formalin (final conc. ca. 4%) for 15 min. Sample coverslips were then rinsed with 5 mL of pure water and then air dried prior to microscopy preparation and analysis.

Atomic Force Microscopy

Atomic force microscopy is an emerging microscopic method that employs a scanning probe for investigating nanoscale biological structures and physical interactions in near-native conditions (Liu and Wang, 2010; Aguayo et al., 2015; Dufrêne et al., 2021; Zhou et al., 2021). Briefly, an ultrasharp tip on a microcantilever is brought into physical contact with a sample surface with actuator movement. The repulsive atomic forces between the AFM tip and sample surface registers as a deflection in the microcantilever, which is measured and monitored by optical beam deflection. Upon contact, the AFM tip images the sample topography by laterally scanning across the surface and maintaining constant force by applying feedback control to adjust tip-sample distance with piezoelectric actuators. In addition to the reconstructed surface topography, the feedback error from the difference between the setpoint force and actual imaging forces can be reconstructed into an error mode image that emphasize sharp changes in the surface.

In non-imaging applications, AFM can measure local force profiles by simultaneously measuring the tip-sample distance and tip forces during extension and retraction movements of the tip with respect to the surface at various spatial points. Adhesive properties can be measured empirically as the maximum attraction force experienced by the tip during its retraction away from the surface. The local deformation of the sample area is measured as the vertical difference between the points of contact in an extension-retraction cycle, where the net tip force is zero. Additionally, energy dissipated from the tip into the sample, a localized mechanical property, can be assessed qualitatively by computing from the difference in integrated area of extension and retraction force-distance curves.

Quantitative Nanomechanical MappingTM (QNM) is a dynamic AFM imaging modality that integrates topographic imaging and nanomechanical characterization (Pittenger and Slade, 2013). Briefly, the AFM tip is sinusoidally oscillated at frequencies higher than image scan rates. In this movement, the tip experiences tapping events of brief contact with the surface at the peak of its movement. The force is monitored during the tapping cycle to measure the peak force applied. Individual tapping cycles are converted into force-distance curves and analyzed to measure sample nanomechanical properties.

Sample coverslips were secured on glass coverslips with adhesive tabs and imaged using a Dimension FastScan Atomic Force Microscope (Bruker, Santa Barbara, CA, United States).

AFM imaging was performed in QNM mode using ScanAsyst-Air probes (Bruker, spring constant: 0.4 N/m, nominal tip radius: 2 nm). Briefly, the AFM tip was oscillated at a PeakForce Tapping frequency of 8 kHz during scanning with a tapping amplitude of 150 nm. Live cell samples were imaged unfixed and in a 0.2- μm syringe-filtered FASW imaging media using ScanAsyst-Fluid Probes (spring constant: 0.7 N/m, tip radius: 20 nm). AFM images were collected at $1,024 \times 1,024$ pixel resolutions at 2 Hz scan rate unless otherwise specified. Raw AFM image data was processed with line flattening and plane fitting routines using Nanoscope Analysis (Bruker) and Gwyddion software¹. For select AFM images, Gwyddion software was used to generate SEM image-like presentations from AFM height data simulated by Monte Carlo integration (Klapetek et al., 2004). The length and width of nanotubes were measured from independent $10 \mu\text{m} \times 10 \mu\text{m}$ image scans, from 2 replicate samples for TW7 and ALTSIO isolates. The frequency of intercellular connections was determined as the number of interconnecting bacterial structures normalized by the number of cells within an AFM image scan. The average frequency was calculated from the harmonic mean of the observed frequencies from regions presenting intercellular connections.

Scanning and Transmission Electron Microscopy

Samples were prepared as specified above on glass coverslips for scanning electron microscopy (SEM) analysis and secured onto a SEM sample holder with carbon tape. Samples were sputter coated with chrome for 3 s and then imaged on a Zeiss Sigma 500 SEM microscope (Zeiss, Thornwood, NY, United States).

Standard negative stain protocols were used to prepare bacterial samples, as specified above, for transmission electron microscopy (TEM) imaging. Briefly, samples were placed in modified Karnovsky's fixative (2.5% glutaraldehyde and 2% paraformaldehyde in 0.15 M sodium cacodylate buffer, pH 7.4) for at least 4 h, postfixed in 1% osmium tetroxide in 0.15 M cacodylate buffer for 1 h and stained en bloc in 2% uranyl acetate for 1 h. Samples were then dehydrated in ethanol, embedded in Durcupan epoxy resin (Sigma-Aldrich), sectioned at 50 to 60 nm on a Leica UCT ultramicrotome, and picked up on Formvar and carbon-coated copper grids. TEM sample grids were viewed on a FEI Tecnai Spirit G2 BioTWIN Transmission Electron Microscope equipped with an Eagle 4k CCD camera (FEI, Hillsboro, OR, United States).

RESULTS

Intercellular Connectivity Between Marine Bacteria

We observed during nanoscale imaging in native-like conditions with AFM numerous instances of bacterial nanotubes connecting cell pairs within surface populations of *Pseudoalteromonas* sp. TW7 and *Alteromonas* sp. ALTSIO cultured isolates. A study

of bacterial nanotubes and their size measurements among TW7 and ALTSIO cells shows variability in their dimensions. **Figure 1** shows representative AFM and SEM images of the various intercellular bacterial nanotubes in TW7 and ALTSIO cultured cells. Nanotubes visually classified from intercellular connections were individually measured from AFM height images ($n = 2$). Histograms of nanotube length and width were derived from 71 nanotubes and are shown in **Figure 1** ($n_{\text{TW7}} = 47$, $n_{\text{ALTSIO}} = 24$). The nanotube lengths range 100–600 nm, and the widths range 50–160 nm (measured by the half maximum width at the connection midpoint). A single outlier case with a length of 918 nm observed in ALTSIO cells was excluded from the length distribution. A single peak was observed in the unimodal observed frequency distributions for nanotube widths, with a peak within the 60–120 nm range, for both ALTSIO and TW7 bacterial isolates (**Figures 1E,G**). The nanotube length distributions differed between TW7 and ALTSIO and were observed as bimodal and unimodal distributions, respectively. Two peaks were observed in TW7 nanotube length distribution (**Figure 1H**), around 150–200 nm and 350–450 nm, with a separation threshold at approximately 250 nm. In comparison, ALTSIO nanotubes had relatively shorter lengths, with a range of 100–350 nm, and the distribution peak between 100 and 200 nm (**Figure 1F**). The heights of bacterial nanotubes between cells range between 18 and 250 nm, where connections >150 nm in width are correlated with a greater height. Nanotubular connections with a measured height less than 100 nm are likely due to the intercellular structure settling on the substrate surface along its span. In addition to nanotubes, there were various observations of wide, short intercellular connections between cells lacking a tubular appearance; such features had widths greater than 150 nm and lengths lower than 250 nm and potentially consist of polymers forming a physical linkage between cells.

Connection Frequency

The average frequency of general intercellular connections per bacterial cell was 0.11 for TW7 ($n_{\text{cells}} = 501$) and 0.07 for ALTSIO ($n_{\text{cells}} = 545$), which include bacterial nanotubes and general physical linkages (i.e., not tubes). The range of observed frequencies in TW7 cells are 0.03–0.68 connections per cell ($n_{\text{images}} = 11$) and in ALTSIO cells are 0.02–0.50 connections per cell ($n_{\text{images}} = 17$). Of these observed intercellular connections, 67% for TW7 ($n_{\text{nanotubes}} = 47$) and 44% for ALTSIO ($n_{\text{nanotubes}} = 24$), were classified as individual nanotubular structures based on reported descriptions, resulting in an average frequency of 0.07 and 0.03 of nanotubes per bacterial cell for the respective bacterial isolates. These connections are classifiable as nanotubes based on singular connection between two cells, a linear span, well-defined edges, and with a consistent width and devoid of deviation along its span.

The cultured isolates have a much higher frequency compared to bacterial cell assemblages from enriched seawater, in which two instances of nanotubes were observed (see **Figure 2**). This observed data is potentially impacted by the misclassification of some observed bacterial nanotubes due to misidentifying physical linkages with the similar physical dimensions and characteristics.

¹<http://gwyddion.net>

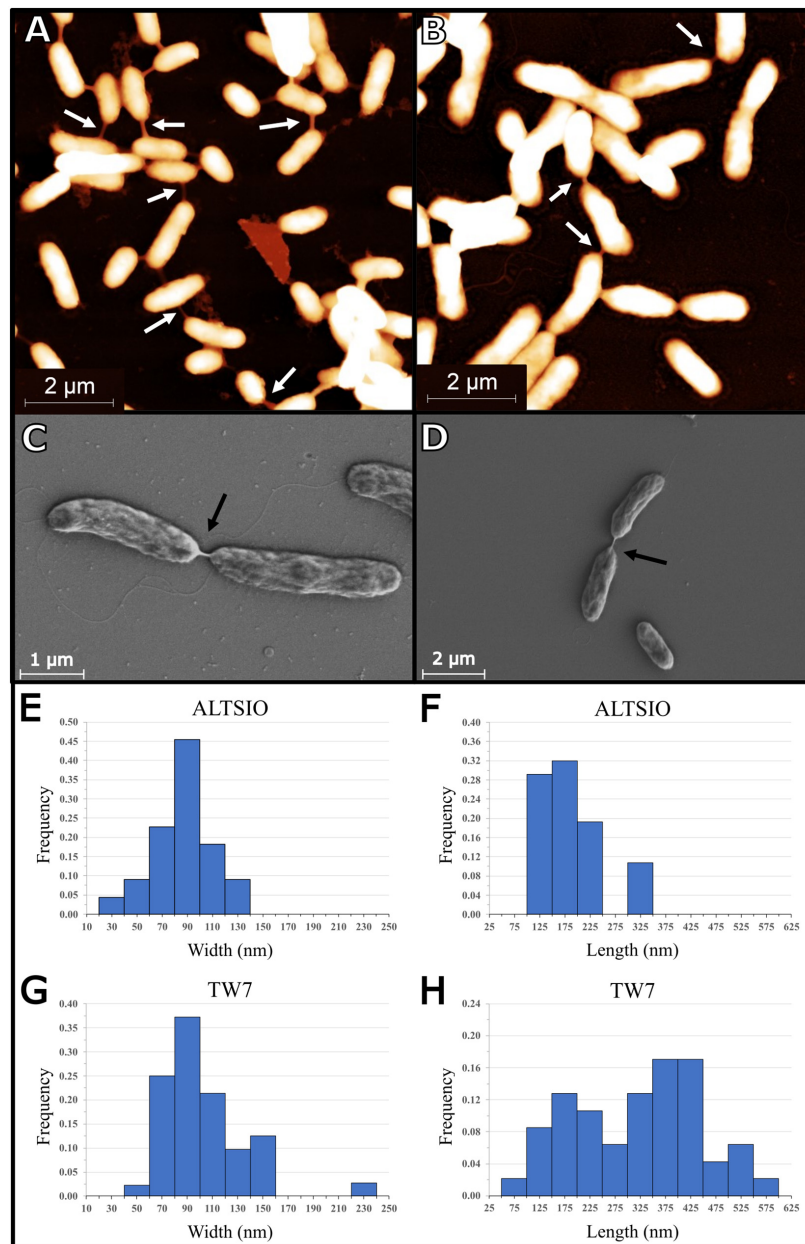


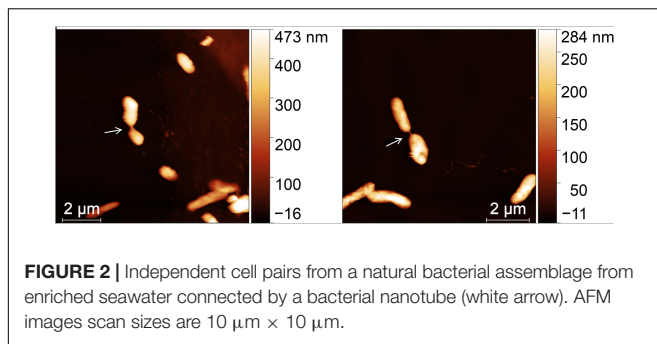
FIGURE 1 | Images of bacterial nanotubes in marine isolates *Pseudoalteromonas* sp. TW7 (A,C) and *Alteromonas* sp. ALTSIO (B,D) reveal various nanotubes and physical connections between adjacent cells (A,B: AFM; C,D: SEM). Observed frequencies of nanotube width and length measurements are shown for ALTSIO (E,F) and TW7 (G,H) cells. Frequency values were calculated from fractions of all ALTSIO ($n = 24$) and TW7 ($n = 47$) nanotubes. Bin sizes for width and length graphs are 20 and 50 nm, respectively.

Bacterial Networks

In AFM images, we observed distributed groups of TW7 cells interconnected via bacterial nanotubes forming a tentative microbial network (Figure 1). Most cells with nanotubes are connected to one or two other cells with few cells connected to more cell partners. Additional representative images of marine bacteria isolates expressing bacterial nanotubes are shown in **Supplementary Figure 2**. AFM topographic images and their representative SEM image-like representations, generated

by Monte Carlo simulation using Gwyddion image analysis software (Klapetek et al., 2004), show other instances of bacterial nanotubular connections and extended interconnectivity found in different groups of TW7 and ALTSIO cells.

Nanotubes can extend bacterial networks beyond single pairs, to longer serial connections of cells and, less frequently, bacterial hubs that connect to multiple cells. Variability in intercellular connections was observed within bacterial cell neighborhoods, with nanotubes and other instances of physical intercellular



connections were also observed connecting cell pairs, as shown in **Supplementary Figure 3**.

In addition to TW7, and ALTSIO cells, nanotube expression was observed in 2 separate α -proteobacterial isolates (La5 and La6) cultured from natural seawater collected from Scripps Pier (San Diego, CA, United States) (**Supplementary Figure 4**). Individual bacterial nanotubes were detected using fluorescence microscopy by co-staining TW7 and ALTSIO cells with NanoOrange and FM 4-64FX to label proteins and lipids, respectively, as shown in **Supplementary Figure 5**. In images processed by a smoothing operation and Mexican hat filter, individual structures appear as faint linear connections between the greater fluorescence intensity of cell membrane regions, with varying labeling efficacy of protein and lipid stains.

Transmission Electron Microscopy Images Showing Membrane Contiguity

Nanotube were observed as contiguous extensions of bacterial cell membrane connecting two cells, with or without intercellular material, in TEM imaging of negatively stained section off TW7 cells, shown in **Figure 3**. An example of paired TW7 cells connected by a bacterial nanotube is shown. This representative connection, with measured length of 250 nm and width of 200 nm, has an interior channel with labeled cellular material that is 100 nm in width. The membrane continuity of nanotubes is suggestive of connected cytoplasmic compartments of participating cells. Cellular material can be shared between the two cells as shown in the TEM images. The measured channel is large enough to support the direct transfer of large cytoplasmic materials, such as large particles, aggregates, and potentially bacterial microcompartments. Nanotubular connections form part of extended cellular connectivity, with occasional material transfer between TW7 cells, as shown in **Supplementary Figure 6** depicting a labeled particle and polymer in transfer between connecting cells.

Physical Characteristics of Nanotubes

We measured the nanomechanical properties of bacterial nanotubes among TW7 cells using the force measuring capabilities of AFM to quantify the maximum adhesion force and energy dissipated at each pixel point. The measured adhesion forces are surface properties that are relevant to the attachment and interaction with biotic and abiotic elements of the marine microenvironment (e.g., colloidal particles and microbial

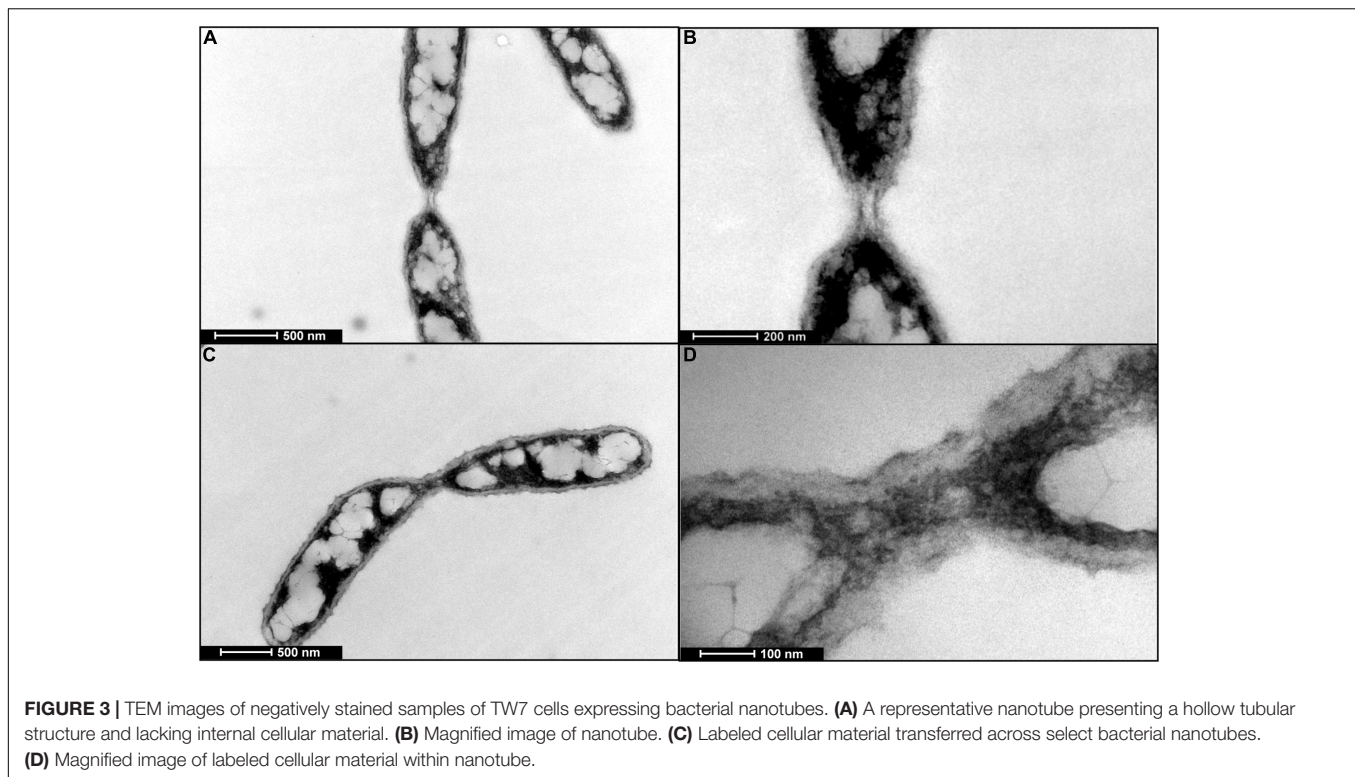
surfaces). The dissipated energy is a qualitative mechanical property quantifying the energy loss in the indentation of the surface, that shows the spatial distribution and relative differences in the viscoelastic properties of the sample surface. **Figure 4** shows the AFM data of TW7 cells, with corresponding error mode, adhesion, and dissipation images, where the nanotubes have varying mechanical properties compared to the connecting cell bodies. Additional nanomechanical data for TW7 cells and nanotubes are shown in **Supplementary Figures 7, 8**. In both figures of nanomechanical images, prominent bacterial nanotubes are present along with other intercellular connections that bear some similarities with nanotubes. The alternate intercellular connections are primarily low-lying structures that resemble nanotubes in their direct span between two cells, with parallel edges and lack kinks or deviations along their length. The low-lying connections are entirely flattened upon the substrate with minimal height profile and present a nanomechanical profile of tubular connections. The adhesion and dissipation data are inconsistent where the edges are comparable to cells and nanotubes with less definition, and the midline properties resemble the substrate. The confounding interstitial features can be misinterpreted as nanotubes from nanomechanical data images but lack the structural definition and physical size of bacterial nanotubes.

Time-lapse fluid imaging of live TW7 cells (**Supplementary Figure 9**) revealed an intercellular nanotube connecting a pair of live cells within a filtered autoclaved seawater medium. The presence of this nanotube suggests that these structural connections between cells can persist for periods of at least 90 min. The measured nanomechanical properties of this nanotube (**Supplementary Figure 9**) appear to be consistent over the duration of imaging and in relation to the properties of the connecting cells, suggesting they do not undergo drastic changes over such periods of time.

This observation indicates that nanotubes can withstand a certain degree of applied AFM scanning forces and tip movement effects, suggesting a level of stability that can potentially hold cells together and move concertedly. Representative line traces of the nanotube (depicted in **Supplementary Figure 9**) height and nanomechanical data are shown and summarily plotted over successive image scans in **Supplementary Figure 10**. The measured nanomechanical data shows slight differences in the adhesion, deformation and dissipation measured relative to the connective connected cell. This can be partially attributed to the influence of the background substrate and the slight differences observed can be obscured by the variability in the intercellular variation in nanomechanical properties. There is little variation in relative nanomechanical property changes relative to the microbial surface properties over time.

Interspecies Bacterial Connections

Bacterial nanotubes were less frequent in natural bacterial assemblages from seawater samples compared to ALTSIO and TW7 marine bacterial isolates. AFM imaging of natural seawater enriched with 1% Marine Broth 2216 shows two unique cell pairs connected by a bacterial nanotube in **Figure 2**. Samples were prepared by cell deposition and fixing the cells in place after 10 min. The incubation period involved in preparation



suggests nanotube production occurs between bacterial cells in suspension instead of stimulated production after cell attachment to the glass surface.

Scanning electron microscopy is an alternative or complementary technique to confirm the presence of nanotubes and for measuring the frequency and occurrence of nanotube connections. In a cell mixture of cultured TW7 cells and cells from enriched natural assemblages (at a 1:1 ratio), SEM images show putative interspecies linkages between morphologically distinct cells, connecting the longer, thinner TW7 bacteria with the smaller, wider natural assemblage bacteria. SEM data shows TW7 cells mixed with that natural assemblage created a microbial network and connected microbial consortium as shown in **Figure 5**. The linkages appear to connect individual cells to a cluster of other cells, holding separate cells together, creating a degree of physical coordination or spatial restriction between the individual cells. Similarly, cell monolayers of natural bacterial assemblages from enriched seawater have multiple instances of small groups of cells with very short intercellular bacterial nanotubes connecting cells of different sizes and shapes as shown in **Figure 6**. Within the close neighborhood of bacterial cells in monolayer, select pairs of cells are connected by bacterial nanotubes as observed in the height and nanomechanical data images.

Structural Variability of Nanotubes and Intercellular Linkages

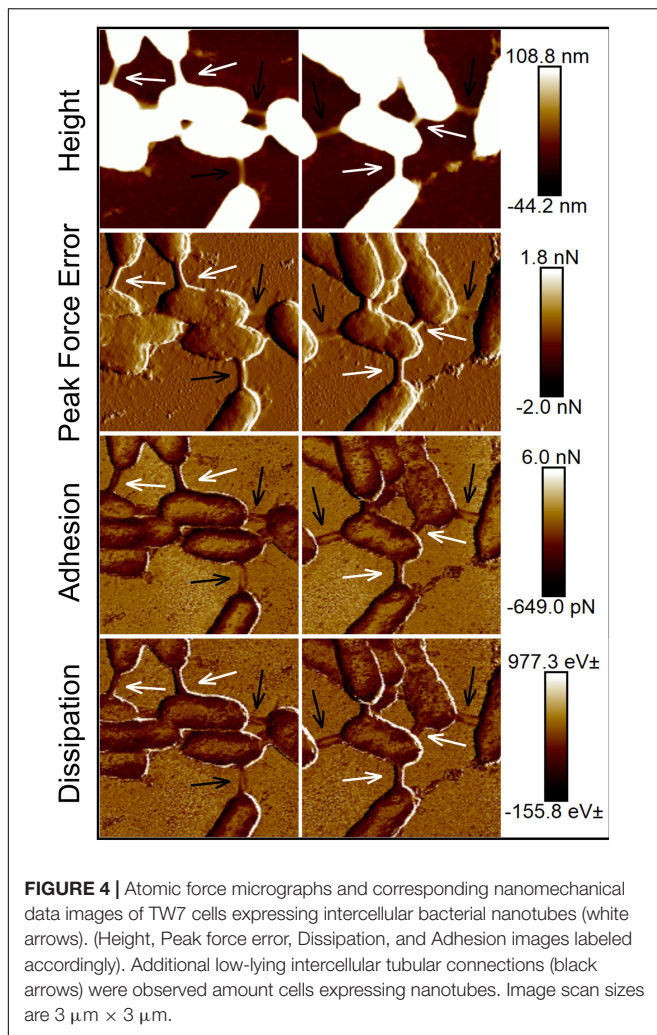
There were two distinct types of intercellular linkages, bacterial nanotubes and other mechanical linkages (i.e., not tubes), that are

distinguished by their shape, quantity and mechanical properties. Individually nanotubes are tubular structures that solely extend between two cells (across $\sim 200\text{--}400$ nm), as opposed to connecting more than two cells. Furthermore, as singular structures, nanotubes position two cells a set distance apart and do not divide or conjoin to form multiple parallel structures. In contrast, mechanical linkages lack a distinct tubular shape, span a shorter distance, form multiple parallel linkages, and promote additional connections to hold cells together, as shown in **Supplementary Figure 11**. Observed adhesion forces and measured dissipation energies on the mechanical linkages were greater compared to the cell surface. Instances of intercellular linkages were observed to coalesce with each other to form contiguous surfaces between adjoining cells (**Supplementary Figure 11**). Additionally, complex arrangements of nanotubes and intercellular linkages were observed in interstitial spaces between cells in larger bacterial networks and aggregates (**Supplementary Figure 12**).

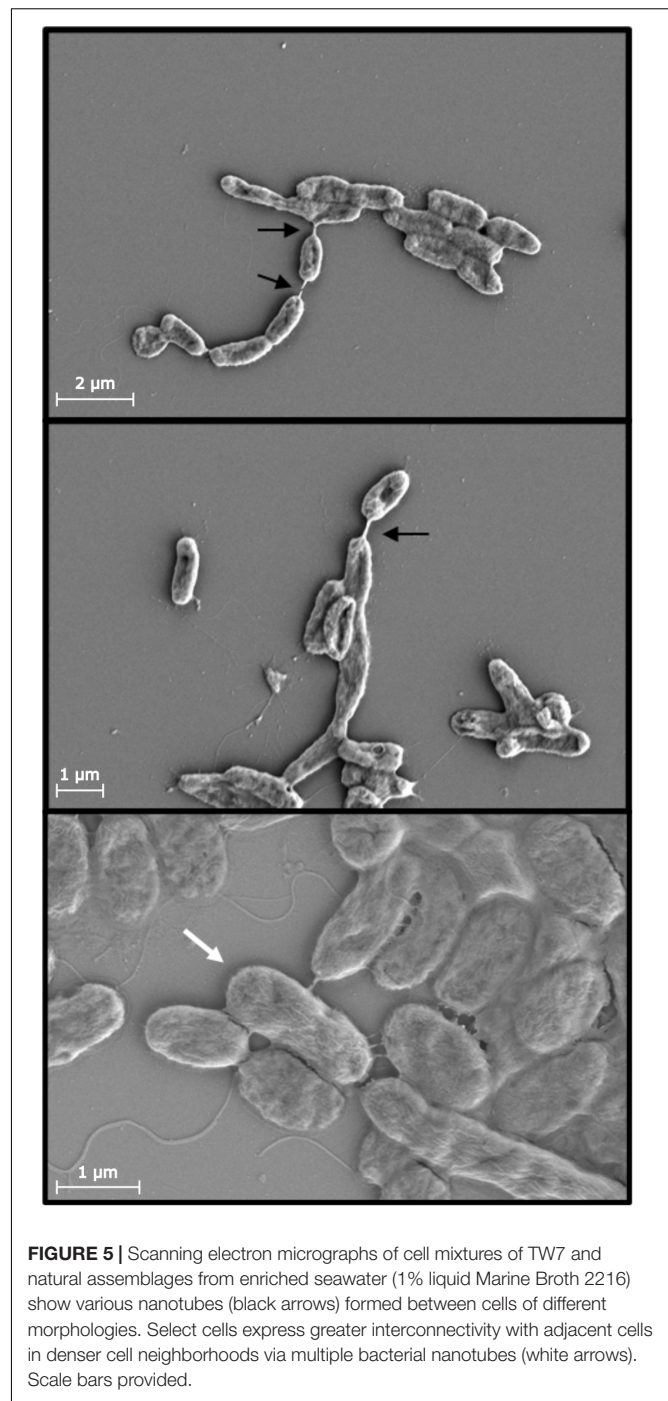
DISCUSSION

Nanotubes Form Intimate Physical Connections Between Marine Bacteria

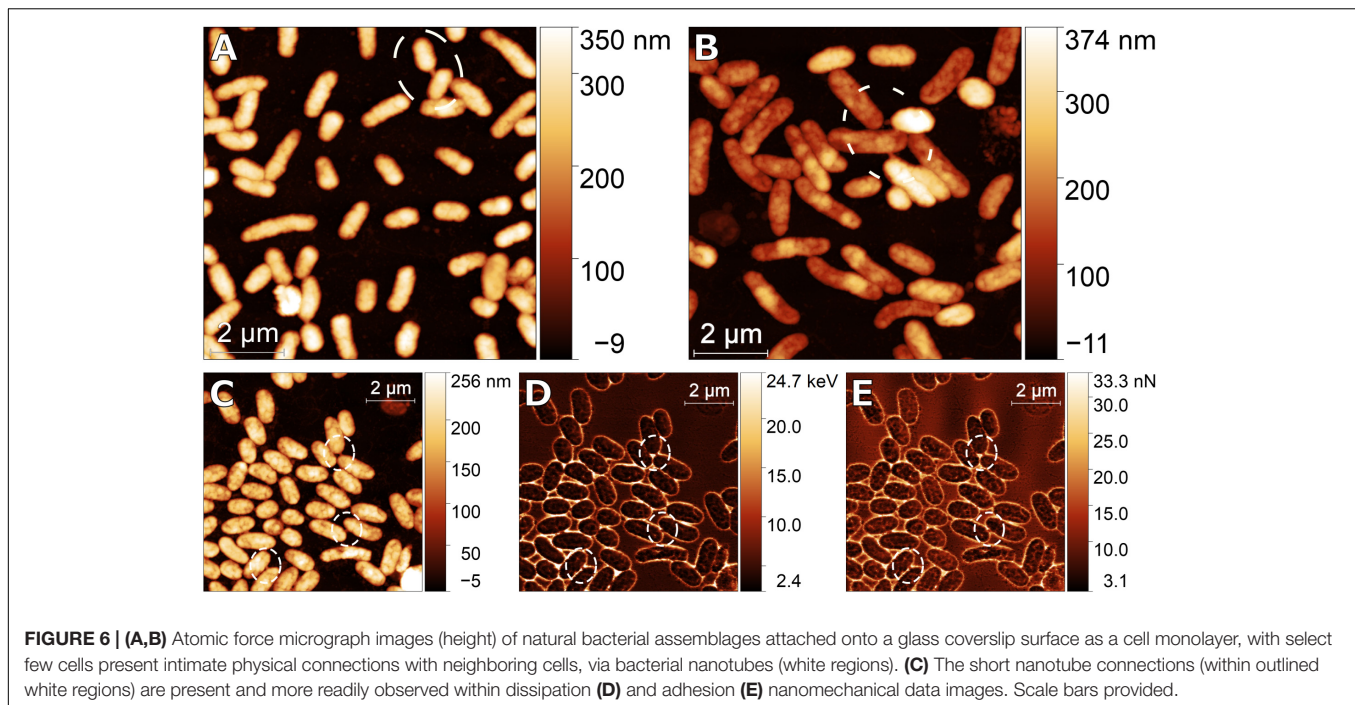
This is the first report of nanotube-based physical connectivity between marine bacteria cells. The compounded connectivity between cell pairs and microbial ensembles contributes to connecting individual cells to denser cell clusters and aggregates over longer spatial scales (>10 μm). The intercellular connections are separable into two categories,



bacterial nanotubes, and more generic mechanical linkages (**Supplementary Figure 3**). Bacterial nanotubes are identifiable from their visual characteristic tubular structure with a linear span and consistent width, devoid of kinks or deviations, as initially observed in *B. subtilis* and *E. coli* cells by Dubey and Ben-Yehuda (2011). Nanotubes are distinguishable from other intercellular connections potentially formed from exopolymers and occupy the interstitial space as observed in archaea (Jahn et al., 2008). From our observations, the widths and lengths of marine bacterial nanotubes fall within the range of 50 – 160 nm and 200 – 600 nm, respectively, with few exceptions, conforming to previous reports by Dubey and Ben-Yehuda (2011). Other generic mechanical linkage connections are generally wider and shorter. The heights along the midsection of the nanotubes range from 18 to 250 nm and could be a potential physical criterion for distinguishing them as bacterial nanotubes, apart from other bacterial structures and appendages. One significant distinction is that in AFM height images other bacterial structures are generally unsupported and tend to lie flat on the background substrate whereas nanotubes are supported at both ends by the two connected bacterial cell bodies.



Nanotubes in marine isolates were ≤ 600 nm long, and much shorter among surface-attached cells from enriched natural bacterial assemblages. The short span of bacterial nanotubes can contribute to a limited overall size of interconnected bacterial networks in an ensemble structure. Such constraints may be more common and significant in marine bacterial isolates compared to *B. subtilis* and *E. coli* nanotubes, which extend up to $1 \mu\text{m}$ (Dubey and Ben-Yehuda, 2011). This implies an upper bound on nanotube length in marine bacteria.



Frequency of Nanotubes

The average frequency of nanotube connections observed in TW7 and ALTSIO were 0.07 and 0.03 nanotube cell⁻¹, respectively. For comparison, general intercellular connections (not-tube) were on average 0.10 and 0.07 connections cell⁻¹ (Figure 1). The frequency of nanotubes was variable from the observed regions (average of ~28 cells per 10 μm × 10 μm area). Apart from few regions of dense interconnectivity as outliers, our frequency range of intercellular connections was 0.02 – 0.10 nanotube cell⁻¹ for surface-attached bacterial isolates in enriched microenvironments. We estimate that our frequency measurements may be 10–100-fold overestimated due to sample preparation selectively removing unattached cells, lacking nanotube expression. On the other hand, sample preparation methods that involve physical processes such as filtration and centrifugation likely disrupt nanotubes and hence contribute to underestimation of nanotube-based cellular connections. The combined influence of high cell seeding density and bacterial surface adsorption via deposition contribute to conditions conducive to intercellular nanotube observation.

In addition to γ -proteobacteria isolates TW7 and ALTSIO, we also tested two cultured α -proteobacteria isolated from seawater from Scripps Pier and found them to be positive for nanotube expression (Supplementary Figure 4). Furthermore, we observed individual bacterial nanotubes connecting cells from enriched natural seawater (Figure 2). We did not conduct a (technically challenging) systematic survey of marine bacteria isolates or natural assemblages for their nanotube expression. However, the protocols developed here lend themselves to expanding the range of species for nanotube expression. It should therefore be possible to test the hypothesis that nanotube expression is a general phenotype expressed within natural

marine assemblages. Our observed frequency of nanotubes in TW7 and ALTSIO isolates was greater compared to seawater assemblages. This could be because some bacterial species have higher relative rates of nanotube expression. But it is more likely due to different nutrient and growth conditions. Thus, a systematic test of the generality of nanotube expression in marine bacteria (or bacteria from any other environment, e.g., as soil or human microbiome) is feasible, technically challenging, but desirable. However, detailed and mechanistic studies of a limited number of isolates or model natural systems should be a priority.

Cytoplasmic Transfer Between Cells via Nanotubes

Previous biochemical and molecular dynamics studies (Dubey and Ben-Yehuda, 2011; Pande et al., 2015) have established that bacterial nanotubes allow for direct exchange of cellular components. Our study is mainly focused on the ecological and biogeochemical implications of nanotube expression taking advantage of the capabilities of multiple imaging modalities. Our TEM images of TW7 nanotubes (Figure 3), show clearly delineated tube boundaries and stained cellular materials within the nanotubes. While not capturing its dynamics, the images are consistent with intercellular transfer of cytoplasmic and/or periplasmic materials between the two cells. We observed varying degrees of negatively stained material within the hollow interior of different nanotubes. Small molecules in bacterial cytoplasm should be readily diffusible across the nanotubes unless there are regulatory mechanisms constraining molecular exchange. Furthermore, the large width of intercellular nanotubes of the intercellular connections (ca. 50 – 160 nm) could accommodate directional transfer between the two cells of components such as protein aggregates and bacterial microcompartments.

Individual cells connecting to cell clusters via a nanotube (e.g., **Figure 1**) may derive benefit from connecting to a cell cluster, potentially gaining access to a pool of greater biochemical diversity. Transmission of metabolites and signaling molecules across nanotube-connected bacterial ensembles could promote biological coordination and synchronicity.

Fluorescence Detection of Nanotube

In addition to AFM visualization, marine bacterial nanotubes in TW7 and ALTSIO samples are detectable to a limited extent using confocal fluorescence microscopy via co-staining proteins and lipids (**Supplementary Figure 5**). Both isolates showed nanotubes labeled by the protein stain NanoOrange; by visual inspection of the fluorescent micrographs, the staining intensity in the nanotubes and the cells was comparable. Only the TW7 cell nanotube was labeled by the lipophilic FM 4-64FX membrane stain, suggesting that the TW7 nanotubes have similar levels of lipid components compared to other cell membrane regions. The differential staining with FM 4-64FX may be due to differences in structure and relative composition of lipophilic and proteinaceous components in nanotubes.

Fluorescence-based detection have limited utility in delineating nanotubes from other labeled membrane regions between marine bacterial cells. The use of non-specific protein and lipid stains is influenced by non-localized fluorescence detection around the connection. Furthermore, overstaining cellular material via non-specific fluorescence labeling limits image contrast of nanotube structures, posing significant challenges for detection in more complex environmental samples with this strategy. Determining specific proteins that are associated with nanotube structures, such as flagellar CORE proteins and YmdB phosphodiesterase, for specific fluorescence targeting may be a viable strategy to enhance discovery rates of nanotubes in marine bacterial assemblages via fluorescent microscopy (Dubey et al., 2016; Bhattacharya et al., 2019). Further studies are needed to refine the ability to detect and observe nanotube structures within marine microenvironments to determine their functionality, development, and ecological significance in marine bacterial communities.

Insights Into Nanomechanical Properties of Bacterial Nanotubes

Multiparametric AFM imaging has potential utility in characterizing bacterial nanotubes using physical characteristics (length and width) and nanomechanical properties (adhesion and dissipation). In general, bacterial nanotubes have defined edges (**Figure 4**, Peak Force Error images), and present lower adhesion and dissipation compared to cell surfaces, and greater contrast from background substrates (**Figure 4**, Adhesion, Dissipation images). Nanomechanical data images can provide better visual contrast for identifying bacterial nanotubes in larger surveyed areas compared to height or peakforce error images (**Supplementary Figures 7, 8A**). In non-ideal conditions, identifying nanotubes associated with other materials and features from topography data can be challenging. Identifying intercellular nanotubes in such cases from characteristic nanomechanical data is desirable, such

as, for example, a potential nanotube structure embedded within interstitial material (**Supplementary Figures 11E–G**). Nanomechanical characterization of bacterial nanotubes can be confounded by additional features such as low-lying interstitial connection, which resemble tubular structures with less distinct edges and inconsistent adhesion and dissipation properties (**Supplementary Figure 8B**). The characterization of bacterial nanotubes is dependent on the physical structures imaged, where freestanding structures are readily identifiable compared to more obscured counterparts. Furthermore, characterization of altered nanotube structures due to development or environmental changes cannot be performed solely from AFM topography data. For example, characterizing the low-lying tubular features that resemble nanotubes (**Figure 4; Supplementary Figure 8B**) and their function in relation to nanotubes cannot be accomplished by AFM imaging. Further investigation is needed to determine how nanomechanical properties of bacterial nanotubes differ among bacterial species and other comparable structures in microbial communities. Further, the protocols developed here could be applied to similar interrogations of bacteria adapted to other environments (e.g., whether salinity of the environment influences the nanomechanical properties of the nanotubes).

Extended Physical Coordination

Bacterial nanotubes influence the physical interactions occurring between two cells, as opposed to indirect coordination and interactions through, e.g., polymers, gel matrices or surfaces. Nanotubes can contribute to the development of a spatial structure within a microbial community by connecting cells and maintaining their relative positions and separation distances over time. Nanotubes were persisted for at least 90 min (**Supplementary Figure 9**) a significant duration in the lives of adjoined bacteria. Nanotube expression can extend the duration of an interaction of bacterial cells and potentially supporting and amplifying and possibly regulating any biological effects of interactions. Interconnected bacterial ensembles can potentially have significant consequences as they move in a concerted manner through a dynamic microenvironment. One possibility is the concerted interaction and attachment of cells to the surfaces of organic particles and polymeric gels. Nanotube based bacteria microaggregates could serve as nuclei for the generation of pre-colonized marine snow (10^8 – 10^9 bacteria mL^{-1}) in coastal marine surface waters by attracting motile bacteria as well as colloids and particles. The concerted metabolic action of nanotube associated bacteria could contribute to the biogeochemical dynamics of marine snow.

Nanotubes expression between interconnected ensembles of bacterial cells presents ecological benefits through functional multicellularity. The interaction extends into physical coordination as bacterial nanotubes establish some degree of ordering and spatial organization of cells, as their positioning and movement within the microenvironment is constrained. The physical network of cells forms a larger interactive biological surface, altering the flow of ambient fluid and promoting interstitial organic matter attachment and buildup between connecting cell bodies (e.g., **Supplementary Figure 12**). Complex intercellular connections formed from multiple parallel nanotubes and intercellular linkages can form an interaction

surface for interstitial particles and polymers and nucleate bacterial aggregates.

Interspecies Connectivity

Interspecies bacterial nanotubes as observed by Dubey and Ben-Yehuda (2011) and by us here raise questions on how common they might be in the ocean, as they can bring together and connect various constituents of marine assemblages. Such connections can build interconnected multispecies bacterial ensembles, as observed from connections between morphologically different cells in SEM and AFM images (Figures 5, 6). These physical intercellular connections could support the spatial and biochemical coupling of different microbial species by allowing for intimate exchange of metabolites and cytoplasmic material across these structures over short spatial scales (<1 μm). Biochemical coupling via bacterial nanotubes of different species has been previously demonstrated in auxotrophic cell mutants exchanging the necessary compounds (Pande et al., 2015). Metabolite interchange and distribution between connected bacterial ensemble may be influenced by nanotube width (ca. 50 – 160 nm), where the interior surface chemistry may provide selective passage of molecules.

Within an interconnected microbial ensemble, nanotubes can form a foundational structure and basis for transient or collapsible bacterial microaggregates, capable of accommodating individual cells into the larger group. Bacterial nanotubes have been shown to be manifested structures associated with cell death, forming due to biophysical forces, with potential altruistic benefits to other neighboring bacteria (Pospíšil et al., 2020). Nanotubes, as manifestations from cell death, can form a scaffold around the released cell contents or surround live cells and promote released organic matter aggregation, generating a hotspot of organic matter. Nanotube expression can provide benefits of transient symbioses to individual cells forming physical connections that accommodate metabolite interchange between members of bacterial assemblages.

Limited Knowledge and Open Questions

Little is known about the structural and physiological characteristics of marine bacterial nanotubes and their ecological role within the marine microenvironment. Production of bacterial nanotubes in *B. subtilis* cells is known to involve the CORE protein complex involved in flagellar production and is associated with YmdB phosphodiesterase activity (Dubey et al., 2016; Bhattacharya et al., 2019). More work is needed to elucidate the conditions and factors necessary for nanotube expression in marine bacteria considering that these structures have only been observed with low frequency among surface-attached cells in our study. This limits our understanding to nanotube structures between surface-attached bacteria and may not directly relate to their formation, development, and mechanisms of actions in planktonic bacteria and natural microenvironments. As back-of-the-envelope calculation with an estimated 10^{29} bacteria in the ocean and a conservative estimated frequency of bacterial nanotubes of 10^{-4} or 10^{-5} , there may be 10^{24} – 10^{25} nanotubes at any given time connecting bacterial cells and forming innumerable interconnected multicellular bacterial ensembles

throughout the ocean. The variability of nanotube expression across bacterial species has significant implications for their relevance in cooperative strategies and multicellular behavior of within mixed communities.

CONCLUSION

In conclusion, the discovery of nanotubes in marine bacteria has novel implications for microbial oceanography and biogeochemistry. Nanotube-mediated exchange of cytoplasmic contents between bacteria changes how we think about the *in situ* physiology and growth regulation of bacteria in the sea. Nanotube-based bacteria-bacteria and bacteria-organic-matter interactions may result in collapsible structures at the microscale. This could enhance the aggregation of microbes and colloidal organic matter and their downward flux in the ocean. Finally, nanotube-based interactions of bacteria in densely populated environments (e.g., marine snow, coral mucus, marine sediments) offers a new view of the biochemical and biogeochemical dynamics within these microenvironments.

DATA AVAILABILITY STATEMENT

The raw data supporting the conclusions of this article will be made available by the authors, without undue reservation.

AUTHOR CONTRIBUTIONS

NP and FA contributed to conception and design of the study. NP performed the data collection, analysis, and wrote the first draft of the manuscript. NP, YY, and FA wrote sections of the manuscript. All authors contributed to manuscript revision, read, and approved the submitted version.

FUNDING

This study was supported by the Gordon and Betty Moore Foundation, Marine Microbiology Initiative (grant 4827) to FA.

ACKNOWLEDGMENTS

We thank Julie Dinasquet for providing α -proteobacteria isolates sp. La5 and La6. We acknowledge Vrinda Sant for help in sample processing and imaging with SEM microscopy. We acknowledge Timo Meerloo and Ying Jones from the UC San Diego Cellular & Molecular Medicine Electron Microscopy Facility for help in preparing negative-stain samples for TEM imaging and help in TEM operating and image acquisition.

SUPPLEMENTARY MATERIAL

The Supplementary Material for this article can be found online at: <https://www.frontiersin.org/articles/10.3389/fmars.2021.768814/full#supplementary-material>

REFERENCES

- Aguayo, S., Donos, N., Spratt, D., and Bozec, L. (2015). Single-bacterium nanomechanics in biomedicine: unravelling the dynamics of bacterial cells. *Nanotechnology* 26:062001. doi: 10.1088/0957-4484/26/6/062001
- Alarcon-Martinez, L., Villafraña-Baughman, D., Quintero, H., Kacerovsky, J. B., Dotigny, F., Murai, K. K., et al. (2020). Interpericyte tunnelling nanotubes regulate neurovascular coupling. *Nature* 585, 91–95. doi: 10.1038/s41586-020-2589-x
- Astanina, K., Koch, M., Jüngst, C., Zumbusch, A., and Kiemer, A. K. (2015). Lipid droplets as a novel cargo of tunnelling nanotubes in endothelial cells. *Sci. Rep.* 5:11453. doi: 10.1038/srep11453
- Azam, F., and Malfatti, F. (2007). Microbial structuring of marine ecosystems. *Nat. Rev. Microbiol.* 5:782. doi: 10.1038/nrmicro1747
- Azam, F., Smith, D., Steward, G., and Hagström, Å (1994). Bacteria-organic matter coupling and its significance for oceanic carbon cycling. *Microb. Ecol.* 28, 167–179. doi: 10.1007/BF00166806
- Baidya, A. K., Rosenshine, I., and Ben-Yehuda, S. (2020). Donor-delivered cell wall hydrolases facilitate nanotube penetration into recipient bacteria. *Nat. Commun.* 11:1938. doi: 10.1038/s41467-020-15605-1
- Benner, R., and Kaiser, K. (2003). Abundance of amino sugars and peptidoglycan in marine particulate and dissolved organic matter. *Limnol. Oceanography* 48, 118–128.
- Bhattacharya, S., Baidya, A. K., Pal, R. R., Mamou, G., Gatt, Y. E., Margalit, H., et al. (2019). A ubiquitous platform for bacterial nanotube biogenesis. *Cell Rep.* 27, 334–342.e10. doi: 10.1016/j.celrep.2019.02.055
- Dubey, G. P., and Ben-Yehuda, S. (2011). Intercellular nanotubes mediate bacterial communication. *Cell* 144, 590–600.
- Dubey, G. P., Malli Mohan, G. B., Dubrovsky, A., Amen, T., Tspishtein, S., Rouvinski, A., et al. (2016). Architecture and characteristics of bacterial nanotubes. *Dev. Cell* 36, 453–461.
- Dufrène, Y. F., Viljoen, A., Mignolet, J., and Mathelié-Guinlet, M. (2021). AFM in cellular and molecular microbiology. *Cell. Microbiol.* 23:e13324.
- Fischer, T., Schorb, M., Reintjes, G., Kolovou, A., Santarella-Mellwig, R., Markert, S., et al. (2019). Biopearling of interconnected outer membrane vesicle chains by a marine flavobacterium. *Appl. Environ. Microbiol.* 85:e00829-19. doi: 10.1128/AEM.00829-19
- Flemming, H.-C., and Wurtz, S. (2019). Bacteria and archaea on Earth and their abundance in biofilms. *Nat. Rev. Microbiol.* 17, 247–260. doi: 10.1038/s41579-019-0158-9
- Goussot, K., Schiff, E., Langevin, C., Marijanovic, Z., Caputo, A., Browman, D. T., et al. (2009). Prions hijack tunnelling nanotubes for intercellular spread. *Nat. Cell Biol.* 11, 328–336. doi: 10.1038/ncb1841
- Green, E. R., and Meccas, J. (2016). Bacterial secretion systems: an overview. *Microbiol Spectr.* 4:10.1128/microbiolspec.VMBF-0012-2015
- Jahn, U., Gallenberger, M., Junglas, B., Eisenreich, W., Stetter, K. O., Rachel, R., et al. (2008). Nanoarchaeum equitans and Ignicoccus hospitalis: new insights into a unique, intimate association of two archaea. *J. Bacteriol.* 190, 1743–1750. doi: 10.1128/JB.01731-07
- Kaiser, K., and Benner, R. (2008). Major bacterial contribution to the ocean reservoir of detrital organic carbon and nitrogen. *Limnol. Oceanography* 53, 99–112. doi: 10.4319/lo.2008.53.1.0099
- Klapetek, P., Necas, D., and Anderson, C. (2004). Gwyddion user guide. *Czech Metrol. Institute* 2007:2009.
- Klein, T. A., Ahmad, S., and Whitney, J. C. (2020). Contact-dependent interbacterial antagonism mediated by protein secretion machines. *Trends Microbiol.* 28, 387–400. doi: 10.1016/j.tim.2020.01.003
- Liu, S., and Wang, Y. (2010). Application of AFM in microbiology: a review. *Scanning* 32, 61–73. doi: 10.1002/sca.20173
- Lukaszczyk, M., Pradhan, B., and Remaut, H. (2019). The biosynthesis and structures of bacterial pili. *Subcell Biochem.* 92, 369–413. doi: 10.1007/978-3-030-18768-2_12
- Pande, S., Shitut, S., Freund, L., Westermann, M., Bertels, F., Colesie, C., et al. (2015). Metabolic cross-feeding via intercellular nanotubes among bacteria. *Nat. Commun.* 6:6238. doi: 10.1038/ncomms7238
- Pelicic, V. (2008). Type IV pili: e pluribus unum? *Mol. Microbiol.* 68, 827–837. doi: 10.1111/j.1365-2958.2008.06197.x
- Pirbadian, S., Barchinger, S. E., Leung, K. M., Byun, H. S., Jangir, Y., Bouhenni, R. A., et al. (2014). *Shewanella oneidensis* MR-1 nanowires are outer membrane and periplasmic extensions of the extracellular electron transport components. *Proc. Natl. Acad. Sci. U S A.* 111, 12883–12888. doi: 10.1073/pnas.1410551111
- Pittenger, B., and Slade, A. (2013). Performing quantitative nanomechanical AFM measurements on live cells. *Microscopy Today* 21, 12–17.
- Pospíšil, J., Vítovská, D., Kofroňová, O., Muchová, K., Šanderová, H., Hubálek, M., et al. (2020). Bacterial nanotubes as a manifestation of cell death. *Nat. Commun.* 11:4963.
- Remis, J. P., Wei, D., Gorur, A., Zemla, M., Haraga, J., Allen, S., et al. (2014). Bacterial social networks: structure and composition of *M. xanthus* outer membrane vesicle chains. *Environ. Microbiol.* 16, 598–610. doi: 10.1111/1462-2920.12187
- Russell, A. B., Peterson, S. B., and Mougous, J. D. (2014). Type VI secretion system effectors: poisons with a purpose. *Nat. Rev. Microbiol.* 12, 137–148. doi: 10.1038/nrmicro3185
- Stempler, O., Baidya, A. K., Bhattacharya, S., Mohan, G. B. M., Tzipilevich, E., Sinai, L., et al. (2017). Interspecies nutrient extraction and toxin delivery between bacteria. *Nat. Commun.* 8:315. doi: 10.1038/s41467-017-00344-7
- Sure, S., Ackland, M. L., Torriero, A. A., Adholeya, A., and Kochar, M. (2016). Microbial nanowires: an electrifying tale. *Microbiology* 162, 2017–2028. doi: 10.1099/mic.0.000382
- Tavi, P., Korhonen, T., Hänninen, S. L., Bruton, J. D., Lööf, S., Simon, A., et al. (2010). Myogenic skeletal muscle satellite cells communicate by tunnelling nanotubes. *J. Cell. Physiol.* 223, 376–383. doi: 10.1002/jcp.22044
- Wakeham, S. G., Pease, T. K., and Benner, R. (2003). Hydroxy fatty acids in marine dissolved organic matter as indicators of bacterial membrane material. *Organ. Geochem.* 34, 857–868. doi: 10.1016/s0146-6380(02)00189-4
- Wells, M. L., and Goldberg, E. D. (1991). Occurrence of small colloids in sea water. *Nature* 353, 342–344. doi: 10.1038/353342a0
- Zark, M., Christoffers, J., and Dittmar, T. (2017). Molecular properties of deep-sea dissolved organic matter are predictable by the central limit theorem: evidence from tandem FT-ICR-MS. *Mar. Chem.* 191, 9–15. doi: 10.1016/j.marchem.2017.02.005
- Zhou, G., Zhang, B., Tang, G., Yu, X.-F., and Galluzzi, M. (2021). Cells nanomechanics by atomic force microscopy: focus on interactions at nanoscale. *Adv. Phys. X* 6:1866668. doi: 10.1080/23746149.2020.1866668

Conflict of Interest: The authors declare that the research was conducted in the absence of any commercial or financial relationships that could be construed as a potential conflict of interest.

Publisher's Note: All claims expressed in this article are solely those of the authors and do not necessarily represent those of their affiliated organizations, or those of the publisher, the editors and the reviewers. Any product that may be evaluated in this article, or claim that may be made by its manufacturer, is not guaranteed or endorsed by the publisher.

Copyright © 2021 Patel, Yamada and Azam. This is an open-access article distributed under the terms of the Creative Commons Attribution License (CC BY). The use, distribution or reproduction in other forums is permitted, provided the original author(s) and the copyright owner(s) are credited and that the original publication in this journal is cited, in accordance with accepted academic practice. No use, distribution or reproduction is permitted which does not comply with these terms.